



ELSEVIER

Available online at www.sciencedirect.com

SCIENCE @ DIRECT®

Inorganica Chimica Acta 348 (2003) 271–278

Inorganica  
Chimica Acta

www.elsevier.com/locate/ica

Note

# Syntheses, spectroscopy and fluxional behavior of the $\eta^3$ -crotyl, $C_3H_4(CH_3)$ , pyrolidinyldithiocarbamate molybdenum complexes: crystal structure of *exo*-[Mo{ $\eta^3$ - $C_3H_4(CH_3)$ }( $\eta^2$ - $S_2CNC_4H_8$ )(CO)( $\eta^2$ -dppm)]

Kuang-Hway Yih<sup>a,\*</sup>, Gene-Hsiang Lee<sup>b</sup>, Shou-Ling Huang<sup>b</sup>, Yu Wang<sup>c</sup><sup>a</sup> Department of Applied Cosmetology, Hung Kuang University, 34 Chung Chi Road, Shalu, Taichung Hsien, Taiwan 433<sup>b</sup> Instrumentation Center, College of Science, National Taiwan University, Taipei, Taiwan 106<sup>c</sup> Department of Chemistry, National Taiwan University, Taipei, Taiwan 106

Received 14 October 2002; accepted 27 November 2002

## Abstract

The *endo*- and *exo*-complexes [Mo{ $\eta^3$ - $C_3H_4(CH_3)$ }( $\eta^2$ - $S_2CNC_4H_8$ )(CO)( $\eta^2$ -diphos)] (diphos: dppm = {bis(diphenylphosphino)methane} (**2**); dppe = {1,2-bis(diphenylphosphino)ethane} (**3**)) are prepared by reacting the 16-electron complex [Mo{ $\eta^3$ - $C_3H_4(CH_3)$ }( $\eta^2$ - $S_2CNC_4H_8$ )(CO)<sub>2</sub>] (**1**) with diphos in refluxing acetonitrile. The orientations of *endo* and *exo* are defined in such a way that the open face of the allyl group and carbonyl group are in the same direction in the former and in the opposite direction in the latter. The variable temperature <sup>1</sup>H NMR was used to confirm that there was no allyl rotation behavior of *endo* ↔ *exo* interconversion of **2** before the thermal decomposition. X-ray crystal structure of *exo*-**2** has been employed to elucidate the *exo* orientation and the methyl moiety of the allyl ligand is found to orient away from the dppm ligand.

© 2003 Elsevier Science B.V. All rights reserved.

**Keywords:** Endo-, *exo*-orientations;  $\eta^3$ -Crotyl molybdenum complexes; Pyrolidinyldithiocarbamate ligand; Crystal structures

## 1. Introduction

The X-ray crystallographic studies [1] and fluxionality [2] of the complexes with [Mo( $\eta^3$ -allyl)(CO)<sub>2</sub>(L<sub>2</sub>)X] (L<sub>2</sub>: pyrazolylborate,  $\beta$ -diketonate, dithiocarbamate, X: neutral monodentate ligand; L<sub>2</sub>: diphos, pyridylphosphane, X: halide) have so far revealed three different solid-state structures as depicted in Fig. 1(A–C) and attributed to the intramolecular trigonal twist (A–B), in which the rotation of the triangular face formed by the L<sub>2</sub>X groups is relative to the face formed by the allyl and the two carbonyl groups. Only a few studies have been focused on the derivatives of complexes [Mo( $\eta^3$ -allyl)(CO)( $\eta^2$ -

S<sub>2</sub>)X]. Recently, we reported the reactions of [Mo( $\eta^3$ -allyl)(CO)<sub>2</sub>( $\eta^2$ -S<sub>2</sub>)X] (S<sub>2</sub> = Et<sub>2</sub>NCS<sub>2</sub>, C<sub>4</sub>H<sub>8</sub>NCS<sub>2</sub>; S<sub>2</sub> = (EtO)<sub>2</sub>PS<sub>2</sub>, X = CH<sub>3</sub>CN) with diphos (diphos = dppm, dppe, dppe) to produce the conformational *endo*-, *exo*-complexes [Mo( $\eta^3$ -C<sub>3</sub>H<sub>5</sub>)( $\eta^2$ -S<sub>2</sub>)(CO)( $\eta^2$ -diphos)] [3] and investigated the rotational behavior of allyl group in these complexes. We have studied the relation of the diphos ligands, the ratios, and free allyl rotational energy of the *endo*-, *exo*-complexes showed the dppe ligand improves the formation of the *endo*-[Mo( $\eta^3$ -C<sub>3</sub>H<sub>5</sub>)( $\eta^2$ -S<sub>2</sub>P(OEt)<sub>2</sub>)(CO)( $\eta^2$ -dppe)] as the sole product [4].

As an extension of our recent work on the stereoselective formation of the sole conformer, we employ crotyl, C<sub>3</sub>H<sub>4</sub>(CH<sub>3</sub>), to investigate the dependence of the ratio and interconversion of the *endo*- and *exo*-conformers.

\* Corresponding author. Fax: +886-4-2632-10-46.

E-mail address: khyih@sunrise.hkc.edu.tw (K.-H. Yih).

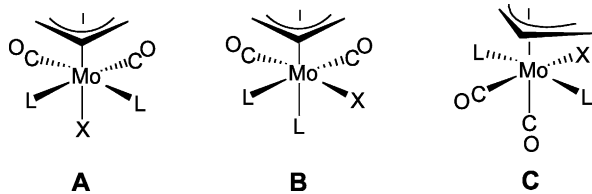


Fig. 1. Three possible structures **A**, **B** and **C** for  $[\text{Mo}(\eta^3\text{-C}_3\text{H}_5)(\text{CO})_2(\text{L}_2)\text{X}]$ .

## 2. Result and discussion

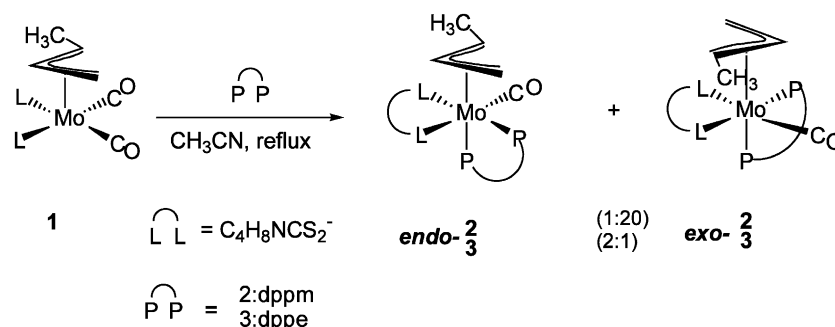
### 2.1. Synthesis of $(\eta^3\text{-crotyl})(\text{dicarbonyl})(\eta^2\text{-pyrolidinylthiocarbamate})\text{molybdenum(II)}$ complex $[\text{Mo}\{\eta^3\text{-C}_3\text{H}_4(\text{CH}_3)\}(\eta^2\text{-S}_2\text{CNC}_4\text{H}_8)(\text{CO})_2]$ (**1**)

Treatment of  $[\text{Mo}(\text{CH}_3\text{CN})_2\{\eta^3\text{-C}_3\text{H}_4(\text{CH}_3)\}(\text{CO})_2\text{-Br}]$  with  $\text{NH}_4(\text{S}_2\text{CNC}_4\text{H}_8)$  in MeOH at room temperature resulted in a replacement reaction, affording the 16-electron complex  $[\text{Mo}\{\eta^3\text{-C}_3\text{H}_4(\text{CH}_3)\}(\eta^2\text{-S}_2\text{CNC}_4\text{H}_8)(\text{CO})_2]$  (**1**) with 88% isolation yield. Preparation of the 16-electron complexes  $[\text{Mo}(\eta^3\text{-allyl})(\text{CO})_2(\eta^2\text{-S}_2\text{CNR})]$  from the reactions of  $[\text{Mo}(\text{CH}_3\text{CN})_2(\eta^3\text{-allyl})(\text{CO})_2\text{Br}]$  with  $\text{NaS}_2\text{CNR}$  ( $\text{R} = \text{C}_4\text{H}_8, \text{Et}_2$ ) have been reported by Shiu et al. [5]. The air-sensitive yellow compound **1** is soluble in polar solvents and insoluble in *n*-hexane and diethyl ether. Complex **1** is more soluble and air-sensitive than the non-methylated complex  $[\text{Mo}(\eta^3\text{-C}_3\text{H}_5)(\eta^2\text{-S}_2\text{CNC}_4\text{H}_8)(\text{CO})_2]$ . The analytical data of **1** are in agreement with the formulation. FAB mass spectrum of **1** shows a parent peak with the typical Mo isotope distribution corresponding to the  $[\text{M}^+]$  molecular mass. The IR spectrum of **1** shows two carbonyl-stretchings with equal intensity, indicating that the two carbonyls are mutually *cis*. Due to the methyl moiety, the room temperature  $^1\text{H}$  NMR spectrum of **1** exhibits five sets of resonances of the  $\text{C}_3\text{H}_4(\text{CH}_3)$  ligand which is typical of the ABCDX spin patterns of unsymmetrical  $\eta^3$ -allyl metal complexes. Only one resonance of the  $\text{H}_{\text{syn}}$  has been observed in  $^1\text{H}$  NMR spectra, which the methyl group occupies the *syn* position of the allyl group (Scheme 1). In the  $^{13}\text{C}\{^1\text{H}\}$  NMR spectrum of **1**, three singlet resonances appear in the carbonyl region. Two relative down-field

singlet resonances at  $\delta$  229.9 and 231.4 are attributed to two chemically non-equivalent carbonyl groups and the relative up-field singlet resonance at  $\delta$  202.0 is assigned to the carbon atom of the  $\text{CS}_2$  of the  $\text{C}_4\text{H}_8\text{NCS}_2$  ligand.

### 2.2. Synthesis of $\text{endo-}$ and $\text{exo-}(\text{carbonyl})(\eta^3\text{-crotyl})(\eta^2\text{-diphos})(\eta^2\text{-pyrolidinylthiocarbamate})\text{-molybdenum(II)}$ complex $[\text{Mo}\{\eta^3\text{-C}_3\text{H}_4(\text{CH}_3)\}(\eta^2\text{-S}_2\text{CNC}_4\text{H}_8)(\text{CO})(\eta^2\text{-dppm})]$ (**2**) and $[\text{Mo}\{\eta^3\text{-C}_3\text{H}_4(\text{CH}_3)\}(\eta^2\text{-S}_2\text{CNC}_4\text{H}_8)(\text{CO})(\eta^2\text{-dppe})]$ (**3**)

The reactions of complexes  $[\text{Mo}(\eta^3\text{-allyl})(\text{CO})_2\text{-(dithio)L}]$  with phenanthroline, phenylacetylene [6] and diphos [3] have been reported. Thus, treatment of  $[\text{Mo}\{\eta^3\text{-C}_3\text{H}_4(\text{CH}_3)\}(\eta^2\text{-S}_2\text{CNC}_4\text{H}_8)(\text{CO})_2]$  (**1**) with dppm or dppe in refluxing acetonitrile yields mixtures of *endo-*, *exo-* $[\text{Mo}\{\eta^3\text{-C}_3\text{H}_4(\text{CH}_3)\}(\eta^2\text{-S}_2\text{CNC}_4\text{H}_8)(\text{CO})(\eta^2\text{-dppm})]$  (**2**) with *endo:exo* ratios of 1:20 or *endo-*, *exo-* $[\text{Mo}\{\eta^3\text{-C}_3\text{H}_4(\text{CH}_3)\}(\eta^2\text{-S}_2\text{CNC}_4\text{H}_8)(\text{CO})(\eta^2\text{-dppe})]$  (**3**) with *endo:exo* ratios of 2:1 (Scheme 1). The air-stable yellow–orange compounds **2** and **3** are soluble in dichloromethane and in acetonitrile and insoluble in diethyl ether and in *n*-hexane. The orientations of *endo* and *exo* are defined to the open face of the allyl group and carbonyl group in the same direction in the former and in the opposite directions in the latter. The spectroscopic and analytical data of **2** and **3** are obtained. In the FAB mass spectra, base peaks with the typical Mo isotope distribution are in good agreement with the  $[\text{M}^+ - \text{CO}]$  molecular masses of **2** and **3**. The IR spectra of **2** and **3** show one terminal carbonyl-stretching band at 1770 and 1790  $\text{cm}^{-1}$ , respectively, although both isomers are known to be present in different ratios. The mixtures of *endo*, *exo*-**2** or *endo*, *exo*-**3** are able to distinguish from different  $^{31}\text{P}\{^1\text{H}\}\text{-}^{31}\text{P}\{^1\text{H}\}$  coupling constants. The  $^{31}\text{P}\{^1\text{H}\}$  NMR spectrum of **2** shows *endo* resonances at  $\delta$  9.7 and 36.1 (with  $^2J(\text{PP}) = 52.1$  Hz) and *exo* resonances at  $\delta$  5.0 and 30.0 (with  $^2J(\text{PP}) = 60.7$  Hz). Compared to the  $^{31}\text{P}\{^1\text{H}\}$  NMR spectrum and the structure of the complex  $[\text{Mo}(\eta^3\text{-C}_3\text{H}_5)(\text{CO})(\eta^2\text{-S}_2\text{CNC}_4\text{H}_8)(\eta^2\text{-dppm})]$  [3], the resonances appear in relative up-field with large coupling constant is assigned to the *exo*-orientation and in the relative down-field



Scheme 1.

with small coupling constant is assigned to the *endo*-orientation. Because of the different ratios of *endo:exo-2* (1:20), the  $^1\text{H}$  and  $^{13}\text{C}\{^1\text{H}\}$  NMR spectra of the major product *exo-2* can be assigned unambiguously from the  $^1\text{H}$ - $^1\text{H}$  COSY and  $^1\text{H}$ - $^{13}\text{C}$  COSY experiments. From Fig. 2, the two *Hanti* protons appear at  $\delta$  2.29 (d,  $^2J(\text{HH}) = 11.7$  Hz) and 2.35 (dd,  $^2J(\text{HH}) = 6.93$  Hz,  $^3J(\text{PH}) = 19.2$  Hz) and the *Hsyn* proton appears at  $\delta$

3.12 ppm, which is overlapped by one proton of the  $\text{NCH}_2$  moiety of the dithiocarbamate ligand. Two resonances are shown at the lowest field in the  $^{13}\text{C}\{^1\text{H}\}$  NMR spectrum of **2**, the relative down-field triplet resonance is attributed to the carbon atom of the carbonyl group that is coupled by two phosphorus atoms and the relative up-field singlet resonance is attributed to the  $\text{CS}_2$  of the dithiocarbamate ligand.

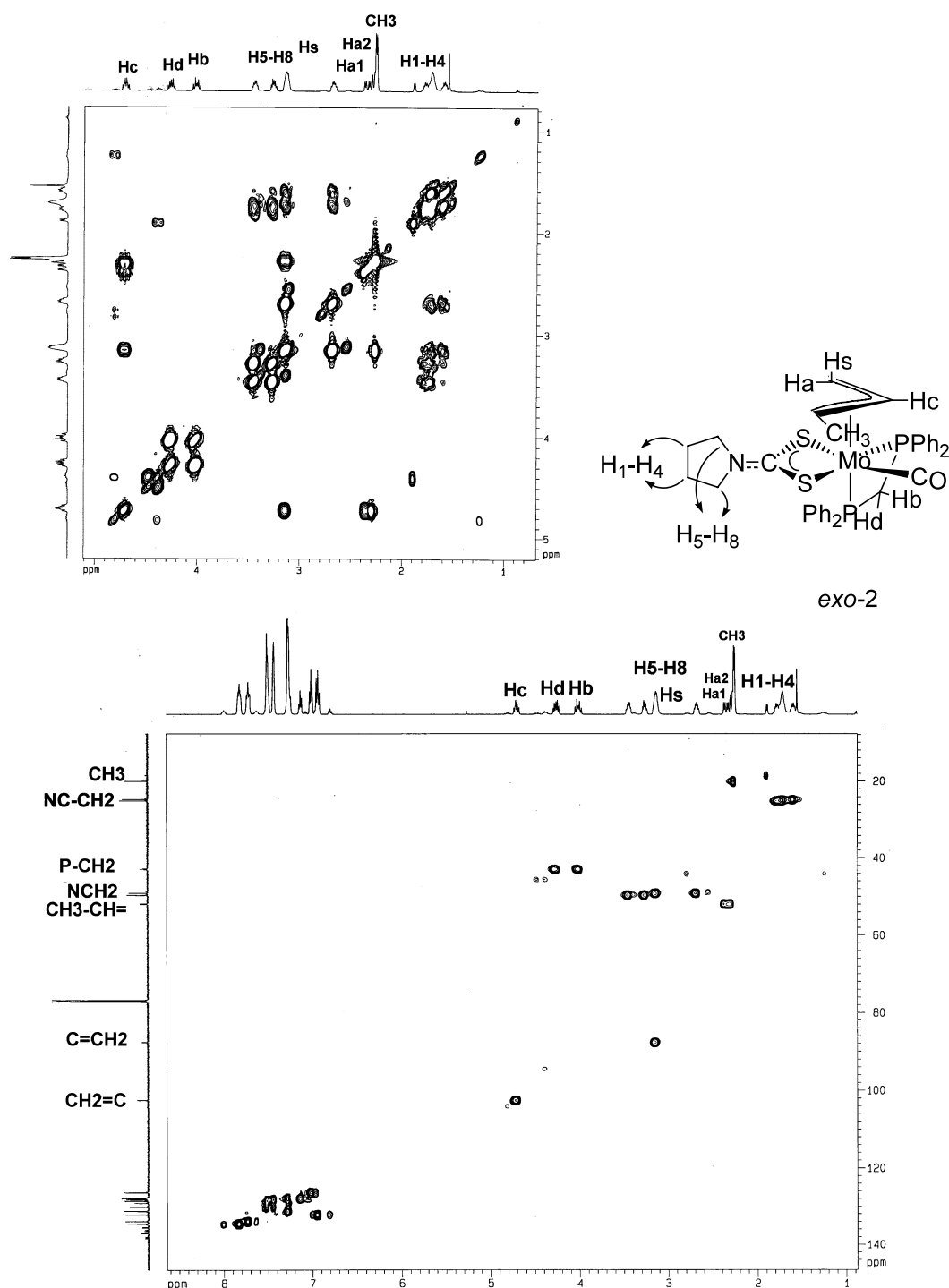


Fig. 2.  $^1\text{H}$ - $^1\text{H}$  COSY and  $^1\text{H}$ - $^{13}\text{C}$  COSY NMR observations of the mixtures *endo*- and *exo-2* in  $\text{CDCl}_3$ .

Compared to the ratios of *endo*-, *exo*-[Mo{ $\eta^3$ -C<sub>3</sub>H<sub>4</sub>(CH<sub>3</sub>)}( $\eta^2$ -S<sub>2</sub>CNC<sub>4</sub>H<sub>8</sub>)(CO)( $\eta^2$ -dppm)] (**2**) (1:20), *endo*-, *exo*-[Mo( $\eta^3$ -C<sub>3</sub>H<sub>5</sub>)( $\eta^2$ -S<sub>2</sub>CNC<sub>4</sub>H<sub>8</sub>)(CO)( $\eta^2$ -dppm)] (1:4) and *endo*-, *exo*-[Mo{ $\eta^3$ -C<sub>3</sub>H<sub>4</sub>(CH<sub>3</sub>)}( $\eta^2$ -S<sub>2</sub>CNC<sub>4</sub>H<sub>8</sub>)(CO)( $\eta^2$ -dppe)] (**3**) (2:1) and *endo*-, *exo*-[Mo( $\eta^3$ -C<sub>3</sub>H<sub>5</sub>)( $\eta^2$ -S<sub>2</sub>CNC<sub>4</sub>H<sub>8</sub>)(CO)( $\eta^2$ -dppe)] (6:1), it is clear that the stereoselective formation of the *exo*-product by the methyl moiety of the allyl ligand is improved.

### 2.3. Variable temperature <sup>1</sup>H and <sup>31</sup>P{<sup>1</sup>H} NMR experiments of *endo*- and *exo*-complex **2**

Variable temperature <sup>1</sup>H NMR experiments can be used to study the fluxional behavior of non-rigid complexes. For example, the rearrangement involving a  $\pi$ - $\sigma$ - $\pi$  [7] process of complexes [Tp'Mo(CO)<sub>2</sub>(allyl)] and intramolecular trigonal twist behavior of complexes [M( $\eta^3$ -C<sub>3</sub>H<sub>5</sub>)(CO)<sub>2</sub>(diphos)I] [8] (M = Mo, W; diphos = dppm, dppe). Recently, we have described the allyl rotational behavior of complexes [Mo( $\eta^3$ -C<sub>3</sub>H<sub>5</sub>)( $\eta^2$ -S<sub>2</sub>CNC<sub>4</sub>H<sub>8</sub>)(CO)( $\eta^2$ -diphos)] (diphos = dppm, dppe). Thus, in order to investigate the fluxionality of the crotyl complex *endo*-, *exo*-**2**, the variable temperature <sup>1</sup>H and <sup>31</sup>P{<sup>1</sup>H} NMR spectra were recorded in the range of 298–328 K. In the range of 298–318 K, the <sup>1</sup>H and <sup>31</sup>P{<sup>1</sup>H} NMR spectra are not changed and the ratio is retained. Surprisingly, the <sup>31</sup>P{<sup>1</sup>H} NMR spectra show only one resonance at  $\delta$  10.2 ppm (Section 4, spectrum A) and the <sup>1</sup>H NMR spectra show organic alkene resonances at  $\delta$  4.8–5.8 at 323 K. From the above description, it is clear that the crotyl group breaks away from the metal complex. The decomposition may be due to the steric hindrance of the crotyl group in the allyl rotational process. Formation of the *endo*-, *exo*-**2** is believed to proceed via one of the phosphorus coordination at the axial position *trans* to the crotyl ligand of **1** to afford a six coordination complex, followed by the crotyl rotation to form the *endo* and *exo* orientations and then the other phosphorus replace the carbonyl group to form the *endo*- and *exo*-**2**.

### 2.4. X-ray structure determination of *exo*-[Mo{ $\eta^3$ -C<sub>3</sub>H<sub>4</sub>(CH<sub>3</sub>)}( $\eta^2$ -S<sub>2</sub>CNC<sub>4</sub>H<sub>8</sub>)(CO)( $\eta^2$ -dppm)] (**2**)

In order to confirm the orientation of the methyl group, we have performed an X-ray diffraction study of **2** at 150 K. The ORTEP plot of **2** is shown in Fig. 3. In the structure, the coordination geometry around the molybdenum atom is approximately an octahedron with the two sulfur atoms, two phosphorus atoms, carbonyl and the crotyl group occupying the six coordination sites. The structure confirms an unequivalent allyl group and the methyl moiety of the allyl ligand is oriented toward CO group. One of the sulfur atoms of dithio ligand is *trans* to the diphos: S(1)–Mo–P(2), 143.93(4)°,

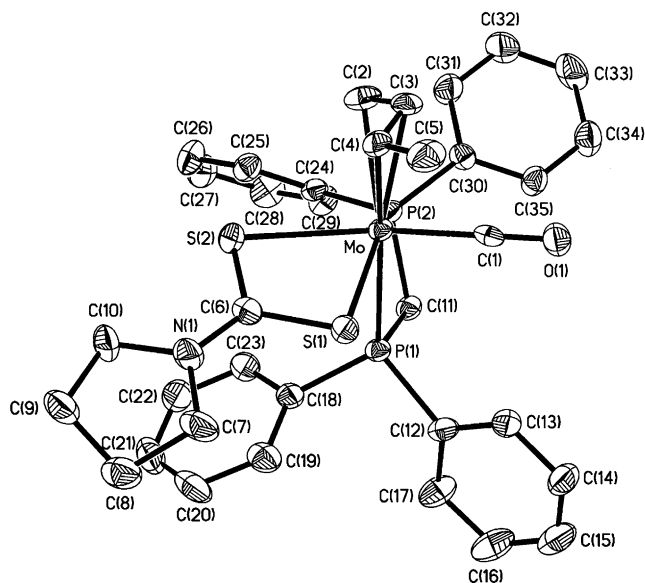


Fig. 3. An ORTEP drawing with 50% thermal ellipsoids and atom-numbering scheme for the complex *exo*-[Mo{ $\eta^3$ -C<sub>3</sub>H<sub>4</sub>(CH<sub>3</sub>)}( $\eta^2$ -S<sub>2</sub>CNC<sub>4</sub>H<sub>8</sub>)(CO)( $\eta^2$ -dppm)] (**2**).

while the other is *trans* to carbonyl: S(2)–Mo–C(1), 169.11(12)°. The S–Mo–S angle of 68.958(17)° in **2** is similar to 68.459(17)° in complex *exo*-[Mo( $\eta^3$ -C<sub>3</sub>H<sub>5</sub>)( $\eta^2$ -S<sub>2</sub>CNC<sub>4</sub>H<sub>8</sub>)(CO)( $\eta^2$ -dppm)] within the experimental errors. The Mo–C(2), C(3) and C(4) bond distances are 2.329(4), 2.337(4) and 2.404(4) Å, respectively. The Mo–S(1) distance of 2.5324(10) Å (*trans* to phosphorus) is clearly shorter than Mo–S(2) of 2.6197(10) Å (*trans* to CO) because of the greater *trans* effect induced by the CO group than the diphos ligand.

The bond distances and intercarbon angle of allyl group in *exo*-**2** (1.393(6), 1.393(6) Å and 120.5(4)°) are in the range of related Mo<sup>II</sup>-allylic compounds (1.31–1.42 Å, 115–125°) [9]. Selected bond distances and angles for *exo*-[Mo{ $\eta^3$ -C<sub>3</sub>H<sub>4</sub>(CH<sub>3</sub>)}( $\eta^2$ -S<sub>2</sub>CNC<sub>4</sub>H<sub>8</sub>)(CO)( $\eta^2$ -dppm)] (**2**) and *exo*-[Mo( $\eta^3$ -C<sub>3</sub>H<sub>5</sub>)( $\eta^2$ -S<sub>2</sub>CNC<sub>4</sub>H<sub>8</sub>)(CO)( $\eta^2$ -dppm)] are listed in Table 3. From this table, the Mo–C1 bond distance of 2.404(4) Å in *exo*-**2** is significantly longer than that of 2.339(2) Å in the non-methylated allyl complex *exo*-[Mo( $\eta^3$ -C<sub>3</sub>H<sub>5</sub>)( $\eta^2$ -S<sub>2</sub>CNC<sub>4</sub>H<sub>8</sub>)(CO)( $\eta^2$ -dppm)] due to the steric hindrance of the methyl moiety.

### 2.5. Conclusion

We employ two diphos ligands and crotyl ligand to investigate the dependence of the ratios and interconversion of the *endo*- and *exo*-conformers. The dppm ligand improves the formation of *exo*-product, whereas the dppe ligand improves the formation of *endo*-product. The *exo*-complexes show large *J*(PP) coupling constant than the *endo*-complexes. The resonances of dppm complex appear in relative up-field for the *exo*-orienta-

tion and dppe complex appear in the relative up-field for the *endo*-orientation. Steric effect of the crotyl ligand improves the formation of *exo*-products and does not induce allyl *endo* ↔ *exo* interconversion of **2** before the thermal decomposition.

### 3. Experimental

#### 3.1. Materials

All manipulations were performed under nitrogen using vacuum-line, drybox, and standard Schlenk techniques. NMR spectra were recorded on an AM-300 or an AM-500 WB FT-NMR spectrometer and are reported in units of parts per million with residual protons in the solvent as an internal standard (CDCl<sub>3</sub>, δ 7.24). IR spectra were measured on a Nicolet Avator-320 instrument and referenced to polystyrene standard, using cells equipped with calcium fluoride windows. MS spectra were recorded on a JEOL SX-102A spectrometer. Solvents were dried and deoxygenated by refluxing over the appropriate reagents before use. *n*-Hexane, diethyl ether, THF and benzene were distilled from sodium-benzophenone. Acetonitrile and dichloromethane were distilled from calcium hydride, and methanol was distilled from magnesium. All other solvents and reagents were of reagent grade and used as received. Elemental analyses and X-ray diffraction studies were carried out at the Regional Center of Analytical Instrument located at the National Taiwan University. Mo(CO)<sub>6</sub> and C<sub>3</sub>H<sub>4</sub>(CH<sub>3</sub>)Br were purchased from Strem Chemical, C<sub>4</sub>H<sub>8</sub>NCS<sub>2</sub>NH<sub>4</sub>, dpmm, and dppe were purchased from Merck.

#### 3.2. ( $\eta^3$ -Crotyl)(dicarbonyl)( $\eta^2$ -pyrolydinyldithiocarbamate)molybdenum(II) complex [Mo{ $\eta^3$ -C<sub>3</sub>H<sub>4</sub>(CH<sub>3</sub>)}( $\eta^2$ -S<sub>2</sub>CNC<sub>4</sub>H<sub>8</sub>)(CO)<sub>2</sub>] (**1**)

MeOH (20 ml) was added to a flask (100-ml) containing NH<sub>4</sub>S<sub>2</sub>CNC<sub>4</sub>H<sub>8</sub> (0.164 g, 1.0 mmol) and [Mo(CH<sub>3</sub>CN)<sub>2</sub>{ $\eta^3$ -C<sub>3</sub>H<sub>4</sub>(CH<sub>3</sub>)}(CO)<sub>2</sub>Br] (0.370 g, 1.0 mmol). The solution was stirred for 5 min at room temperature, and a yellow–orange solids **1** were formed which were isolated by filtration (G4), washed with *n*-hexane (2 × 10 ml) and subsequently drying under vacuum yielding [Mo{ $\eta^3$ -C<sub>3</sub>H<sub>4</sub>(CH<sub>3</sub>)}( $\eta^2$ -S<sub>2</sub>CNC<sub>4</sub>H<sub>8</sub>)(CO)<sub>2</sub>] (**1**) (0.31 g, 88%). Further purification was accomplished by recrystallization from 1/10 CH<sub>2</sub>Cl<sub>2</sub>/*n*-hexane. Spectroscopic data of **1** are as follows. IR (KBr, cm<sup>-1</sup>): ν(CO) 1927(vs), 1851(vs). <sup>1</sup>H NMR (500 MHz, CDCl<sub>3</sub>, 298 K): δ 1.10 (d, <sup>3</sup>J(HH) = 9.2 Hz, 1H, *Hanti*), 1.64 (m, 1H, *Hanti*), 1.80 (d, <sup>4</sup>J(HH) = 6.3 Hz, 3H, CH<sub>3</sub>), 1.91 (s, 4H, NCH<sub>2</sub>CH<sub>2</sub>), 2.94 (d, <sup>3</sup>J(HH) = 6.4 Hz, 1H, *Hsyn*), 3.52 (s, 4H, NCH<sub>2</sub>), 3.75 (m, 1H, *Hc*). <sup>13</sup>C{<sup>1</sup>H} NMR (75 MHz, CDCl<sub>3</sub>, 298 K): δ 18.5 (s,

CH<sub>3</sub>), 24.7 (s, NCH<sub>2</sub>CH<sub>2</sub>), 50.2 (s, NCH<sub>2</sub>), 55.0, 73.5 (s, =CH<sub>2</sub>), 77.0 (s, =CH), 202.0 (s, NCS<sub>2</sub>), 229.9, 231.4 (s, CO). MS (FAB, NBA, *m/z*) 355 (*M*<sup>+</sup>), 327 (*M*<sup>+</sup> – CO), 299 (*M*<sup>+</sup> – 2CO). Anal. Calc. for C<sub>11</sub>H<sub>15</sub>NO<sub>2</sub>S<sub>2</sub>Mo: C, 37.39; H, 4.28; N, 3.97%. Found: C, 37.42; H, 4.40; N, 3.88%.

#### 3.3. *Endo*-, *exo*-(carbonyl)( $\eta^3$ -crotyl)( $\eta^2$ -diphos)( $\eta^2$ -pyrolydinyldithiocarbamate)molybdenum(II) complex [Mo{ $\eta^3$ -C<sub>3</sub>H<sub>4</sub>(CH<sub>3</sub>)}( $\eta^2$ -S<sub>2</sub>CNC<sub>4</sub>H<sub>8</sub>)(CO)( $\eta^2$ -dpmm)] (**2**)

MeCN (20 ml) was added to a flask (100-ml) containing dpmm (0.384 g, 1.0 mmol) and [Mo{ $\eta^3$ -C<sub>3</sub>H<sub>4</sub>(CH<sub>3</sub>)}( $\eta^2$ -S<sub>2</sub>CNC<sub>4</sub>H<sub>8</sub>)(CO)<sub>2</sub>] (**1**) (0.353 g, 1.0 mmol). The solution was refluxed for 1 h, and an IR spectrum indicated completion of the reaction. After removal of the solvent in vacuo, the residue was redissolved with CH<sub>2</sub>Cl<sub>2</sub> (10 ml). *n*-Hexane (15 ml) was added to the solution and a yellow–orange solids *endo*-, *exo*-**2** were formed which were isolated by filtration (G4), washed with *n*-hexane (2 × 10 ml) and subsequently drying under vacuum yielding *endo*-, *exo*-[Mo{ $\eta^3$ -C<sub>3</sub>H<sub>4</sub>(CH<sub>3</sub>)}( $\eta^2$ -S<sub>2</sub>CNC<sub>4</sub>H<sub>8</sub>)(CO)( $\eta^2$ -dpmm)] (**2**) (0.62 g, 87%). Further purification was accomplished by recrystallization from 1/10 CH<sub>2</sub>Cl<sub>2</sub>/*n*-hexane. Spectroscopic data of *endo*-, *exo*-**2** are as follows. IR (KBr, cm<sup>-1</sup>): ν(CO) 1770(vs). MS (FAB, NBA, *m/z*) 721.5 (*M*<sup>+</sup> – CO). Anal. Calc. for C<sub>35</sub>H<sub>37</sub>NOP<sub>2</sub>S<sub>2</sub>Mo: C, 59.23; H, 5.26; N, 1.97%. Found: C, 59.56; H, 5.10; N, 1.84%. <sup>31</sup>P{<sup>1</sup>H} NMR (202 MHz, CDCl<sub>3</sub>, 298 K): *endo*-**2**: δ 9.7, 36.1 (d, <sup>2</sup>J(PP) = 52.1 Hz, dpmm). *exo*-**2**: δ 5.0, 30.0 (d, <sup>2</sup>J(PP) = 60.7 Hz, dpmm). <sup>1</sup>H NMR (500 MHz, CDCl<sub>3</sub>, 298 K): δ 1.60, 1.75, 1.77, 1.78 (m, 4H, NCH<sub>2</sub>CH<sub>2</sub>), 2.26 (d, <sup>4</sup>J(HH) = 5.60 Hz, 3H, CH<sub>3</sub>), 2.29 (d, <sup>3</sup>J(HH) = 11.7 Hz, 1H, *Hanti*), 2.35 (dd, <sup>3</sup>J(HH) = 6.93 Hz, <sup>3</sup>J(PH) = 19.2 Hz, 1H, *Hanti*), 2.68, 3.12, 3.26, 3.44 (m, 4H, NCH<sub>2</sub>), 3.12 (br, 1H, *Hsyn*), 4.01 (dt, <sup>2</sup>J(HH) = 15.1 Hz, <sup>2</sup>J(PH) = 9.0 Hz, 1H, PCH<sub>2</sub>), 4.26 (dd, <sup>2</sup>J(HH) = 15.1 Hz, <sup>2</sup>J(PH) = 8.4 Hz, 1H, PCH<sub>2</sub>), 4.70 (m, 1H, *Hc*). <sup>13</sup>C{<sup>1</sup>H} NMR (125 MHz, CDCl<sub>3</sub>, 298 K): δ 20.0 (s, CH<sub>3</sub>), 24.5, 24.9 (s, NCH<sub>2</sub>CH<sub>2</sub>), 42.9 (t, *J*(PC) = 19.4 Hz, PCH<sub>2</sub>), 48.7, 49.5 (s, NCH<sub>2</sub>), 51.9 (d, <sup>2</sup>J(PC) = 15.1 Hz, CHCH<sub>3</sub>), 87.6 (d, <sup>2</sup>J(PC) = 9.6 Hz, CH<sub>2</sub>=CH), 102.5 (s, CH<sub>2</sub>=CH), 126.3–134.5 (Ph), 204.8 (s, CS<sub>2</sub>), 228.3 (t, <sup>2</sup>J(PC) = 12.6 Hz, CO).

#### 3.4. *Endo*-, *exo*-(carbonyl)( $\eta^3$ -crotyl)( $\eta^2$ -diphos)( $\eta^2$ -pyrolydinyldithiocarbamate)molybdenum(II) complex [Mo{ $\eta^3$ -C<sub>3</sub>H<sub>4</sub>(CH<sub>3</sub>)}( $\eta^2$ -S<sub>2</sub>CNC<sub>4</sub>H<sub>8</sub>)(CO)( $\eta^2$ -dppe)] (**3**)

Complex *endo*-, *exo*-[Mo{ $\eta^3$ -C<sub>3</sub>H<sub>4</sub>(CH<sub>3</sub>)}( $\eta^2$ -S<sub>2</sub>CNC<sub>4</sub>H<sub>8</sub>)(CO)( $\eta^2$ -dppe)] (**3**) was synthesized using the same procedure as that used in the synthesis of **2** by employing **1** and dppe. The yields are 95% for **3**.

Spectroscopic data of *endo*-, *exo*-**3** are as follows. IR (KBr,  $\text{cm}^{-1}$ ):  $\nu(\text{CO})$  1790(vs).  $^1\text{H}$  NMR (500 MHz,  $\text{CDCl}_3$ , 298 K):  $\delta$  1.46, 1.59, 1.66 (m, 4H,  $\text{NCH}_2\text{CH}_2$ ), 1.98 (s, 3H,  $\text{CH}_3$ ), 2.08 (d,  $^4J(\text{HH})$  6.06 Hz, 2H, *Hanti*), 2.25 (br, 1H,  $H_{\text{syn}}$ ), 2.76, 2.85, 3.25 (m, 4H,  $\text{NCH}_2$ ), 2.49, 2.98 (m, 4H,  $\text{PCH}_2$ ), 4.06 (m, 1H, *Hc*).  $^{13}\text{C}\{^1\text{H}\}$  NMR (75 MHz,  $\text{CDCl}_3$ , 298 K):  $\delta$  18.8, 19.7 (s,  $\text{CH}_3$ ), 24.6, 24.9 (s,  $\text{NCH}_2\text{CH}_2$ ), 26.2 (t,  $J(\text{PC}) = 19.8$  Hz,  $\text{PCH}_2$ ), 48.7, 49.2 (s,  $\text{NCH}_2$ ), 77.2 (s,  $\text{CH}_2=\text{CH}$ ), 88.6 (s,  $\text{CH}_2=\text{CH}$ ), 125.4–136.1 (Ph), 203.8, 205.7 (s,  $\text{CS}_2$ ). MS (FAB, NBA,  $m/z$ ) 697.7 ( $M^+ - \text{CO}$ ). *Anal.* Calc. for  $\text{C}_{36}\text{H}_{39}\text{NOP}_2\text{S}_2\text{Mo}$ : C, 59.74; H, 5.43; N, 1.94%. Found: C, 59.66; H, 5.20; N, 1.78%.  $^{31}\text{P}\{^1\text{H}\}$  NMR (202 MHz,  $\text{CDCl}_3$ , 298 K): *endo*-**3**:  $\delta$  56.2, 85.0 (br, dppm). *exo*-**3**:  $\delta$  65.0, 88.3 (d,  $^2J(\text{PP}) = 29.8$  Hz, dppm).

### 3.5. X-ray crystallography

Single crystal of *exo*-**2** suitable for X-ray diffraction analysis was grown by recrystallization from 20/1 *n*-hexane/ $\text{CH}_2\text{Cl}_2$ . The diffraction data were collected at room temperature on an Enraf–Nonius CAD4 diffractometer equipped with graphite-monochromated Mo K $\alpha$  ( $\lambda = 0.71073$  Å) radiation. The raw intensity data were converted to structure factor amplitudes and their esd's after corrections for scan speed, background, Lorentz, and polarization effects. An empirical absorption cor-

rection, based on the azimuthal scan data, was applied to the data. Crystallographic computations were carried out on a Microvax III computer using the NRCC-SDPVAX structure determination package [10].

A suitable single crystal of **2** was mounted on the top of a glass fiber with glue. Initial lattice parameters were determined from 24 accurately centered reflections with  $\theta$  values in the range from 2.08 to 27.50°. Cell constants and other pertinent data were collected and are recorded in Table 1. Reflection data were collected using the  $\theta/2\theta$  scan method. The  $\theta$  scan angle was determined for each reflection according to the equation  $0.70 \pm 0.35 \tan \theta$ . Three check reflections were measured every 30-min throughout the data collection and showed no apparent decay. The merging of equivalent and duplicate reflections gave a total of 26013 unique measured data, of which 7347 reflections with  $I > 2\sigma(I)$  were considered. The first step of the structure solution used the heavy-atom method (Patterson synthesis), which revealed the positions of metal atoms. The remaining atoms were found in a series of alternating difference Fourier maps and least-squares refinements. The quantity minimized by the least-squares program was  $w(|F_o| - |F_c|)^2$ , where  $w$  is the weight of a given operation. The analytical forms of the scattering factor tables for the neutral atoms were used [11]. The non-hydrogen atoms were

Table 1

Crystal data and refinement details for complex *exo*- $[\text{Mo}\{\eta^3\text{-C}_3\text{H}_4(\text{CH}_3)\}(\eta^2\text{-S}_2\text{CNC}_4\text{H}_8)(\text{CO})(\eta^2\text{-dppm})]$  (**2**)

Empirical formula	$\text{C}_{35}\text{H}_{37}\text{NOP}_2\text{S}_2\text{Mo}$
Formula weight	709.66
Crystal system	Trigonal
Crystal size (mm)	$0.28 \times 0.25 \times 0.15$
Space group	$P3_1$
$a$ (Å)	11.2966(1)
$b$ (Å)	11.2966(1)
$c$ (Å)	22.6575(2)
$\gamma$ (°)	120
$V$ (Å <sup>3</sup> )	2504.02(4)
$Z$	3
$T$ (K)	150(1)
$D_{\text{calc}}$ ( $\text{g cm}^{-3}$ )	1.412
$\mu$ (Mo K $\alpha$ ) ( $\text{mm}^{-1}$ )	0.642
$F(000)$	1098
$\theta$ Range	2.08–27.50
$h, k, l$ range	$-14 \rightarrow 14, -14 \rightarrow 14, -29 \rightarrow 26$
Reflections collected	26013
Observed data [ $I > 2\sigma(I)$ ]	7347
No. of parameters	398
$R^a$	0.040
$R_w^b$	0.090
Transmission (min, max)	0.911, 0.824
Quality-of-fit <sup>c</sup>	1.064
$\Delta(D\text{-map})$ max, min ( $e \text{ \AA}^{-3}$ )	$-0.594; 0.774$

<sup>a</sup>  $R = \sum ||F_o| - |F_c|| / \sum |F_o|$ .

<sup>b</sup>  $R_w = [\sum \omega(|F_o| - |F_c|)^2]^{1/2}$ ;  $\omega = 1/\sigma^2(|F_o|)$ .

<sup>c</sup> Quality-of-fit =  $[\sum \omega(|F_o| - |F_c|)^2 / (N_{\text{reflections}} - N_{\text{parameters}})]^{1/2}$ .

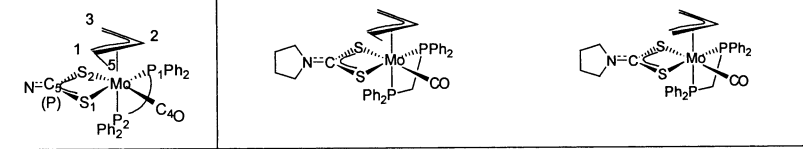
Table 2

Selected bond distances (Å) and angles (°) for *exo*- $[\text{Mo}\{\eta^3\text{-C}_3\text{H}_4(\text{CH}_3)\}(\eta^2\text{-S}_2\text{CNC}_4\text{H}_8)(\text{CO})(\eta^2\text{-dppm})]$  (**2**)

Bond distances			
Mo–S(1)	2.5324(10)	C(2)–C(3)	1.393(6)
Mo–S(2)	2.6197(10)	C(3)–C(4)	1.393(6)
Mo–C(1)	1.902(4)	C(4)–C(5)	1.495(6)
Mo–C(2)	2.329(4)	C(1)–O(1)	1.185(5)
Mo–C(3)	2.337(4)	P(1)–C(11)	1.841(4)
Mo–C(4)	2.404(4)	P(2)–C(11)	1.838(4)
Mo–P(1)	2.4754(10)	S(1)–C(6)	1.726(4)
Mo–P(2)	2.4298(10)	S(2)–C(6)	1.704(4)
C(6)–N(1)	1.333(5)		
Bond angles			
S(1)–Mo–S(2)	68.68(3)	S(1)–C(6)–S(2)	115.9(2)
S(1)–Mo–C(1)	100.52(12)	S(1)–C(6)–N(1)	122.0(3)
S(1)–Mo–C(2)	135.58(10)	S(2)–C(6)–N(1)	122.1(3)
S(1)–Mo–C(3)	113.30(12)	S(1)–Mo–P(2)	143.93(4)
S(1)–Mo–C(4)	79.51(10)	S(1)–Mo–P(1)	77.55(3)
S(2)–Mo–C(1)	169.11(12)	S(2)–Mo–P(1)	89.81(3)
S(2)–Mo–C(2)	86.4(12)	S(2)–Mo–P(2)	101.74(3)
S(2)–Mo–C(3)	101.30(11)	C(1)–Mo–P(1)	89.13(11)
S(2)–Mo–C(4)	84.82(10)	C(1)–Mo–P(2)	87.86(12)
C(1)–Mo–C(2)	101.12(16)	P(1)–Mo–P(2)	67.48(3)
C(1)–Mo–C(3)	81.35(15)	P(1)–C(11)–P(2)	95.58(18)
C(1)–Mo–C(4)	91.93(15)	C(5)–C(4)–Mo	70.3(2)
C(2)–Mo–P(1)	140.78(11)	C(6)–N(1)–C(7)	123.9(4)
C(2)–Mo–P(2)	75.11(10)	C(6)–N(1)–C(10)	123.4(4)
C(3)–Mo–P(2)	102.60(12)	Mo–S(2)–C(6)	86.40(14)
C(4)–Mo–P(1)	156.83(10)	Mo–S(1)–C(6)	88.79(14)
C(3)–Mo–P(1)	166.63(11)	C(7)–N(1)–C(10)	112.2(4)
C(4)–Mo–P(2)	135.68(10)	Mo–C(1)–O(1)	178.6(3)

Table 3

Selected bond distances (Å) and angles (°) for *exo*-[Mo( $\eta^3$ -C<sub>3</sub>H<sub>4</sub>(CH<sub>3</sub>))( $\eta^2$ -S<sub>2</sub>CNC<sub>4</sub>H<sub>8</sub>)(CO)( $\eta^2$ -dppm)] (2) and *exo*-[Mo( $\eta^3$ -C<sub>3</sub>H<sub>5</sub>)( $\eta^2$ -S<sub>2</sub>CNC<sub>4</sub>H<sub>8</sub>)(CO)( $\eta^2$ -dppm)]

		
Bond Distances (Å)		
C <sub>1</sub> -C <sub>2</sub>	1.393(6)	1.398(4)
C <sub>2</sub> -C <sub>3</sub>	1.393(6)	1.377(4)
Mo-C <sub>1</sub>	2.404(4)	2.339(2)
Mo-C <sub>2</sub>	2.337(4)	2.325(2)
Mo-C <sub>3</sub>	2.329(4)	2.369(2)
Mo-C <sub>4</sub>	1.902(4)	1.916(2)
Mo-P <sub>1</sub>	2.4298(10)	2.4336(5)
Mo-P <sub>2</sub>	2.4754(10)	2.4439(5)
Mo-S <sub>1</sub>	2.5324(10)	2.5467(6)
Mo-S <sub>2</sub>	2.6197(10)	2.6181(6)
C <sub>5</sub> -S <sub>1</sub>	1.726(4)	1.726(2)
C <sub>5</sub> -S <sub>2</sub>	1.704(4)	1.709(2)
N-C <sub>5</sub>	1.333(5)	1.324(3)
Bond Angles (°)		
C <sub>1</sub> -C <sub>2</sub> -C <sub>3</sub>	120.5(4)	120.9(3)
P <sub>1</sub> -Mo-P <sub>2</sub>	67.48(3)	67.890(17)
S <sub>1</sub> -Mo-S <sub>2</sub>	68.958(17)	68.459(17)
S <sub>1</sub> -C <sub>5</sub> -S <sub>2</sub>	115.9(2)	115.53(12)
S <sub>1</sub> -Mo-P <sub>1</sub>	143.93(4)	141.421(19)
S <sub>2</sub> -Mo-C <sub>4</sub>	169.11(12)	170.48(7)
Mo-C <sub>4</sub> -O	178.6(3)	178.4(2)

refined anisotropically. Hydrogen atoms were included in the structure factor calculations in their expected positions on the basis of idealized bonding geometry but were not refined in least squares. The final residuals of this refinement were  $R = 0.040$  and  $R_w = 0.090$ . Selected bond distances and angles are listed in Table 2.

#### 4. Supplementary material

Tables of complete atomic coordinates, bond lengths and angles, thermal parameters (4 pages) and listing of

structure factors (15 pages) are available from the author K.H. Yih upon request.

#### Acknowledgements

We thank the National Science Council of the Republic of China for support.

#### References

- [1] (a) R.H. Fenn, A.J. Graham, *J. Organomet. Chem.* 37 (1972) 137;  
(b) A.J. Graham, D. Akrigg, B. Sheldrick, *Cryst. Struct. Com-*

- mun. 24 (1985) 173;  
(c) F.A. Cotton, C.A. Murillo, B.R. Stults, *Inorg. Chim. Acta* 7 (1977) 503;  
(d) C.A. Cosky, P. Ganis, G. Avatibile, *Acta Crystallogr. B* 27 (1971) 1859;  
(e) J.W. Faller, D.F. Chodos, D. Katahira, *J. Organomet. Chem.* 187 (1980) 227;  
(f) F.A. Cotton, M. Jeremic, A. Shaver, *Inorg. Chim. Acta* 6 (1972) 543.
- [2] (a) A.J. Graham, R.H. Fenn, *J. Organomet. Chem.* 17 (1969) 405;  
(b) A.J. Graham, R.H. Fenn, *J. Organomet. Chem.* 25 (1970) 173;  
(c) F.A. Cotton, B.A. Frenz, A.G. Stanislawski, *Inorg. Chim. Acta* 7 (1973) 503;  
(d) F. Dewans, J. Dewailly, J. Meunier-Piret, P. Piret, *J. Organomet. Chem.* 76 (1974) 53.
- [3] K.H. Yih, G.H. Lee, S.L. Huang, Y. Wang, *Organometallics* 21 (2002) 5767.
- [4] K.H. Yih, G.H. Lee, Y. Wang, *Inorg. Chem. Commun.* 3 (2000) 458.
- [5] K.B. Shiu, K.H. Yih, S.L. Wang, F.L. Liao, *J. Organomet. Chem.* 420 (1991) 359.
- [6] K.H. Yih, G.H. Lee, S.L. Huang, Y. Wang, *J. Organomet. Chem.* 658 (2002) 191.
- [7] (a) S.K. Chowdhury, M. Nandi, V.S. Joshi, A. Sarkar, *Organometallics* 16 (1997) 1806 (and references cited therein);  
(b) M. Kollmar, B. Goldfuss, M. Reggelin, F. Rominger, G. Helmchen, *Chem. Eur. J.* 7 (2001) 4913.
- [8] J.W. Faller, D.A. Haitko, R.D. Adams, D.F. Chodos, *J. Am. Chem. Soc.* 101 (1979) 865.
- [9] (a) R.H. Fenn, A.J. Graham, *J. Organomet. Chem.* 37 (1972) 137;  
(b) A.J. Graham, D. Akrigg, B. Sheldrick, *Cryst. Struct. Commun.* 24 (1976) 173;  
(c) F.A. Cotton, C.A. Murillo, B.R. Stults, *Inorg. Chim. Acta* 7 (1977) 503;  
(d) C.A. Cosky, P. Ganis, G. Avatibile, *Acta Crystallogr. B* 27 (1971) 1859;  
(e) J.W. Faller, D.F. Chodos, D. Katahira, *J. Organomet. Chem.* 187 (1980) 227;  
(f) F.A. Cotton, M. Jeremic, A. Shaver, *Inorg. Chim. Acta* 6 (1972) 543.
- [10] E.J. Gabe, F.L. Lee, Y. Lepage, G.M. Sheldrick, C. Kruger, R. Goddard (Eds.), *Crystallographic Computing 3*, Clarendon Press, Oxford, 1985, p. 167.
- [11] (a) *International Tables for X-ray Crystallography* vol. IV, Reidel, Dordrecht, 1974;  
(b) Y. LePage, E. Gabe, *J. Appl. Crystallogr.* 23 (1990) 406.